

## RESEARCH ARTICLE

WILEY

# Cortical gray to white matter signal intensity ratio as a sign of neurodegeneration and cognition independent of $\beta$ -amyloid in dementia

Xiaomeng Xu<sup>1</sup>  | Ikbeom Jang<sup>2,3,4</sup> | Junfang Zhang<sup>1</sup> | Miao Zhang<sup>5</sup> | Lijun Wang<sup>1</sup> | Guanyu Ye<sup>1</sup> | Aonan Zhao<sup>1</sup> | Yichi Zhang<sup>1</sup> | Biao Li<sup>5</sup> | Jun Liu<sup>1,6</sup> | Binyin Li<sup>1,6</sup>  | for the Alzheimer's Disease Neuroimaging Initiative

<sup>1</sup>Department of Neurology and Institute of Neurology, Ruijin Hospital, Shanghai Jiao Tong University School of Medicine, Shanghai, China

<sup>2</sup>Athinoula A. Martinos Center for Biomedical Imaging, Massachusetts General Hospital, Charlestown, Massachusetts, USA

<sup>3</sup>Department of Radiology, Harvard Medical School, Boston, Massachusetts, USA

<sup>4</sup>Division of Computer Engineering, Hankuk University of Foreign Studies, Yongin, South Korea

<sup>5</sup>Department of Nuclear Medicine, Ruijin Hospital, Shanghai Jiao Tong University School of Medicine, Shanghai, China

<sup>6</sup>Clinical Neuroscience Center, Ruijin Hospital, Shanghai Jiao Tong University School of Medicine, Shanghai, China

## Correspondence

Binyin Li, Department of Neurology and Institute of Neurology, Ruijin Hospital, Shanghai Jiao Tong University School of Medicine, Shanghai, 200025, China.  
Email: [libinyin@126.com](mailto:libinyin@126.com)

Jun Liu, Department of Neurology and Institute of Neurology, Ruijin Hospital, Shanghai Jiao Tong University School of Medicine, Shanghai, 200025, China.  
Email: [jly0520@hotmail.com](mailto:jly0520@hotmail.com)

## Funding information

National Natural Science Foundation of China, Grant/Award Numbers: 81901180, 82271441; Shanghai Rising-Star Program, Grant/Award Number: 21QA1405800; National Institutes of Health, Grant/Award Number: U01

## Abstract

Cortical gray to white matter signal intensity ratio (GWR) measured from T1-weighted magnetic resonance (MR) images was associated with neurodegeneration and dementia. We characterized topological patterns of GWR during AD pathogenesis and investigated its association with cognitive decline. The study included a cross-sectional dataset and a longitudinal dataset. The cross-sectional dataset included 60 cognitively healthy controls, 61 mild cognitive impairment (MCI), and 63 patients with dementia. The longitudinal dataset included 26 participants who progressed from cognitively normal to dementia and 26 controls that remained cognitively normal. GWR was compared across the cross-sectional groups, adjusted for amyloid PET. The correlation between GWR and cognition performance was also evaluated. The longitudinal dataset was used to investigate GWR alteration during the AD pathogenesis. Dementia with  $\beta$ -amyloid deposition group exhibited the largest area of increased GWR, followed by MCI with  $\beta$ -amyloid deposition, MCI without  $\beta$ -amyloid deposition, and controls. The spatial pattern of GWR-increased regions was not influenced by  $\beta$ -amyloid deposits. Correlation between regional GWR alteration and cognitive decline was only detected among individuals with  $\beta$ -amyloid deposition. GWR showed positive correlation with tau PET in the left supramarginal, lateral occipital gyrus, and right middle frontal cortex. The longitudinal study showed that GWR increased around the fusiform, inferior/superior temporal lobe, and entorhinal cortex in MCI and progressed to larger cortical regions after progression to AD. The spatial pattern of GWR-increased regions was independent of  $\beta$ -amyloid deposits but overlapped with tauopathy. The GWR can serve as a promising biomarker of neurodegeneration in AD.

Xiaomeng Xu and Jang Ikbeom contributed equally to this work.

This is an open access article under the terms of the [Creative Commons Attribution-NonCommercial-NoDerivs](https://creativecommons.org/licenses/by-nc-nd/4.0/) License, which permits use and distribution in any medium, provided the original work is properly cited, the use is non-commercial and no modifications or adaptations are made.

© 2023 The Authors. *Human Brain Mapping* published by Wiley Periodicals LLC.

AG024904; Department of Defense,  
Grant/Award Number: W81XWH-12-2-0012

**KEYWORDS**

cognitive decline, dementia, GWR, imaging biomarker,  $\beta$ -amyloid

## 1 | INTRODUCTION

Alzheimer's disease (AD) is the most common cause of dementia. It is estimated that brain pathological and morphological changes begin potentially a decade or more prior to the development of clinical symptoms. The recent publication of the National Institute on Aging-Alzheimer's Association (NIA-AA) workgroup suggested biomarker framework of AD as the AT[N] framework, which referred to  $\beta$ -amyloid ( $A\beta$ ), tau, and neurodegeneration respectively (Jack et al., 2018). Neurodegeneration biomarkers, such as hippocampal atrophy and cortical thickness, provide clinicians and researchers with a non-invasive, feasible, and less expensive option to detect AD. Recent advancements in high-resolution MRI, as demonstrated by studies conducted by Jang et al. (2022) and Westlye et al. (2009), enable the detection of altered tissue signal properties of brain microstructure even at earlier phases of pathogenesis. These advances in MRI technology can provide additional information on neurodegeneration beyond traditional neurodegeneration biomarkers. Furthermore, novel imaging data analysis algorithm, such as multiple machine learning models presented in our previous research (Li et al., 2020, 2021), further optimized the accuracy, sensitivity, and specificity in the quantitative evaluation of neurodegeneration biomarkers.

The gray to white matter signal intensity ratio (GWR) is a measurement of tissue property acquired by MRI that reveals tissue intensity contrast. This value is calculated by the ratio of intensity signal of gray matter to white matter. In T1-weighted MRI scans, T1 relaxation times differs between tissues due to the difference in tissue microstructure properties and cell water/lipid content, resulting in higher signal in white matter and lower signal in gray matter (Jefferson et al., 2015; Westlye et al., 2009). Therefore, neurobiological process of aging and diseases that affects tissue microstructure or cell content, such as myelin degradation, axonal loss, and iron deposit, can result in altered regional or global T1 relaxation times. Consequently, these changes lead to altered tissue contrast along the gray/white matter borderline, affecting the GWR (Kim et al., 2002; Salat et al., 2011; Westlye et al., 2009). Previous studies demonstrated that GWR altered with aging (Salat et al., 2009) and cognitive decline in healthy elders (Salat et al., 2011; Westlye et al., 2009). Additionally, Jefferson et al. (2015) found that GWR can predict the conversion from mild cognitive impairment (MCI) to AD, suggesting that GWR may reflect early alterations in brain microstructure, and can serve as a promising biomarker of AD in the early stage. Longitudinal changes in GWR were shown to improve AD prediction as well (Grydeland et al., 2013). In our recent study,

we employed a strategy called multi-scale structural mapping (MSSM) to combined GWRs obtained from multiple layers of the cortex and subcortical white matter with cortical morphometry maps (i.e., MSSM). This approach allowed us to accurately detect patients with AD dementia as well as individuals with MCI who subsequently progressed to AD dementia within the next 3 years (Jang et al., 2022).

Although GWR-based machine learning models could help to classify AD with  $A\beta$  pathology, previous studies mainly looked at the predictive value of the global GWR rather than regional GWR. In the current study, we aimed to investigate the correlation between regional GWR and local AD biomarker accumulation, as well as cognitive performance, using vertex-wise correlation analysis. Our study covered a wide range of dementia by including patients with heterogeneous cognition and  $A\beta$  background (MCI  $A\beta+$ , MCI  $A\beta-$ , AD  $A\beta+$ , and dementia  $A\beta-$ ). In addition, we used a longitudinal cohort to depict the dynamic evolution of GWR in parallel to AD pathogenesis for better understanding of GWR in the neurodegenerative process of AD continuum.

## 2 | METHODS

### 2.1 | Participants

#### 2.1.1 | Cross-sectional dataset

Participants were recruited from the memory clinic in Ruijin Hospital, Shanghai Jiao Tong University School of Medicine. All participants were initially screened by the Mini-Mental State Examination (MMSE, Chinese Version) (Katzman et al., 1988), global clinical dementia rating (CDR = 0.5 for MCI and >0.5 for AD diagnosis), self-rating anxiety/depression scale and activity of daily living questionnaire. Demographics included sex, age, race, and education level. The enrolled participants underwent neuropsychological tests including the Beijing version of the Montreal Cognitive Assessment (MoCA) and the Chinese version of Addenbrooke's Cognitive Examination-Revised (ACER) with subtests of verbal memory, language, attention, fluency, and visual-spatial processing (Fang et al., 2014). Structural MRI and  $A\beta$  PET data were acquired in the same day (Table 1). A subset of participants also had tau PET within 2 weeks (see Appendix S1 for details).

Based on medical history, neuropsychologic performance and  $A\beta$  PET (cut-off for amyloid positivity: cortical-to-whole-cerebellum standardized uptake value ratio 1.11 (Landau et al., 2012)) as suggested by

**TABLE 1** Characteristics and demographics of the cross-sectional dataset.

	CN A $\beta$ –, N = 48	CN A $\beta$ +, N = 12	MCI A $\beta$ –, N = 29	MCI A $\beta$ +, N = 32	Dementia A $\beta$ –, N = 7	AD A $\beta$ +, N = 56	<i>p</i> *
Age (years)	65.0 ± 7.9	71.4 ± 5.7 <sup>a</sup>	69.0 ± 6.8	69.7 ± 9.2	67.7 ± 4.7	66.1 ± 9.3	.059
Education (years)	13.6 ± 2.9	13.7 ± 2.8	11.7 ± 3.6	13.6 ± 2.7 <sup>b</sup>	10.3 ± 2.7	11.1 ± 3.9	.001
Female, <i>n</i> (%)	28 (58.3%)	6 (50%)	17 (58.6%)	17 (53.1%)	4 (57.1%)	29 (51.8%)	.648
MMSE	29.6 ± 0.5	29.6 ± 0.5	26.5 ± 1.6	26.4 ± 1.5	18.3 ± 5.9	17.6 ± 5.3	<.001
MoCA	28.7 ± 1.5	26.2 ± 1.9 <sup>a</sup>	24.8 ± 3.5	23.2 ± 3.4	15.1 ± 6.8	12.1 ± 5.6	<.001
ACER	94.8 ± 4.6	91.3 ± 4.8 <sup>a</sup>	84.1 ± 8.3	81.0 ± 9.7	52.7 ± 22.0	47.7 ± 18.5	<.001
ACER attention	17.8 ± 0.4	18.0 ± 0.1	16.1 ± 1.4	16.2 ± 1.5	11.6 ± 4.9	10.2 ± 3.5	<.001
ACER memory	24.4 ± 2.3	22.7 ± 2.2 <sup>a</sup>	19.6 ± 4.4	16.8 ± 5.6 <sup>b</sup>	8.5 ± 4.6	6.4 ± 4.6	<.001
ACER fluency	11.4 ± 1.9	10.1 ± 1.6 <sup>a</sup>	9.4 ± 2.5	9.5 ± 2.1	4.1 ± 3.3	5.1 ± 3.2	<.001
ACER language	25.4 ± 1.4	24.6 ± 1.7	23.5 ± 3.0	23.2 ± 3.0	17.3 ± 6.0	16.7 ± 6.4	<.001
ACER visuospatial	15.7 ± 0.6	15.8 ± 0.5	15.1 ± 1.6	15.2 ± 1.8	11.1 ± 5.5	9.1 ± 4.9	<.001

Note: Values represented mean ± standard deviation unless otherwise specified.

Abbreviations: ACER, Addenbrooke's Cognitive Examination Revised; AD, Alzheimer's disease; CN, cognitively normal; MCI, mild cognitive impairment; MMSE, Mini-Mental State Examination; MOCA, Montreal Cognitive Assessment.

<sup>a</sup>Significance of differences between CN A $\beta$ – and CN A $\beta$ +

<sup>b</sup>Significance of differences between MCI A $\beta$ – and MCI A $\beta$ +

\**p* value in the analysis of variance between CN, MCI A $\beta$ +, and AD A $\beta$ +

AD research framework, the participants were grouped as the following: cognitively normal with negative A $\beta$  (CN A $\beta$ –), preclinical AD (CN A $\beta$ –), MCI with negative A $\beta$  (MCI A $\beta$ –), MCI with positive A $\beta$  (MCI A $\beta$ –), AD with dementia (AD A $\beta$ –), and dementia with negative A $\beta$  (Dementia A $\beta$ –).

The present study was approved by the ethics committee, Ruijin Hospital, Shanghai Jiao Tong University School of Medicine, China. All participants in the study or their caregivers signed written informed consent after fully understanding the procedure involved.

## 2.1.2 | Longitudinal dataset

To validate the results from our cross-sectional dataset, we acquired longitudinal T1-weighted images of 26 participants from the Alzheimer's Disease Neuroimaging Initiative (ADNI) dataset ([adni.loni.usc.edu](http://adni.loni.usc.edu)). The participants were clinically normal at baseline and progressed to MCI and then dementia in the follow-up (CN-MCI-AD group). Data at baseline, at the first MCI diagnosis, and at the first dementia diagnosis were included for the longitudinal analysis. The mean time interval was 56.8 months (range: 6–108 months) from cognitively normal to MCI and 86.8 months (range: 24–156 months) from normal to dementia. We evaluated the longitudinal GWR changes during AD development. For comparison, we included another 26 cognitive normal participants from ADNI who had three visits with matched baseline cognitive performance and matched time interval between visits to the CN-MCI-Dementia group (Table 2). These participants were evaluated as cognitively normal in all three visits (CN-CN-CN group).

**TABLE 2** Baseline demographics of the CN-CN-CN and CN-MCI-Dementia.

	CN-CN-CN	CN-MCI-Dementia	<i>p</i>
Sample size	26	26	
Female, <i>n</i> (%)	13 (50%)	16 (61.5%)	.402
Baseline age (years)	74.14 ± 4.05	74.89 ± 3.67	.485
Education (years)	16.69 ± 2.98	15.65 ± 2.45	.176
ApoE $\epsilon$ 4 carrier, <i>n</i> (%)	5 (19.2%)	13 (50%)	.020
MMSE	29.08 ± 1.20	29.54 ± 0.71	.097
ADAS-Cog13	8.06 ± 3.96	9.72 ± 4.5	.166
RAVLT immediate	44.46 ± 7.95	44.46 ± 8.74	.999
RAVLT learning	6.35 ± 2.67	5.88 ± 2.60	.530

Abbreviations: ADAS-Cog, the Alzheimer's Disease Assessment Scale-Cognition; CN, cognitively normal participants; MCI, mild cognitive impairment; MMSE, Mini-Mental State Examination; RAVLT, Rey Auditory Verbal Learning Test.

## 2.2 | PET and MRI acquisition

For our cross-sectional dataset, MRI data were acquired in a whole-body PET/MR scanner (Biograph mMR; Siemens Healthcare, Erlangen, Germany) with a standard 8-channel head coil. The T1-weighted three-dimensional structural images were simultaneously acquired with TR = 1900 ms, TE = 2.44 ms, and 192 slices covering the whole brain with voxel size = 1.0 × 1.0 × 1.0 mm<sup>3</sup>.

PET scans using an <sup>18</sup>F florbetapir (FBP) tracer to image A $\beta$  were simultaneously performed. The participants received an intravenous injection of FBP at a mean dose of 3.7 MBq/kg body weight (Li

et al., 2021). Static FBP-PET data were acquired in sinogram mode for 15 min using the following parameters: 128 slices (gap, 0.5 mm) covering the whole brain; FOV, 500 mm; matrix size,  $344 \times 344$ ; voxel size,  $2.6 \times 2.6 \times 3.1 \text{ mm}^3$ , reconstructed with high-definition (HD) PET (21 subsets, 4 iterations) and post-filtered with an isotropic full-width half-maximum (FWHM) Gaussian kernel of 2 mm. Attenuation correction for PET was performed using MR-based attenuation maps derived from a dual-echo Dixon-based sequence.

For ADNI longitudinal dataset, MRI was performed on 3.0 T scanners with the following parameters described by ADNI MRI protocols: Siemens 3D Magnetization Prepared-Rapid Gradient Echo (MPRAGE), TR = 2300 ms, TE = 2.98 ms, flip angle = 90, and voxel size =  $1.0 \times 1.0 \times 1.0 \text{ mm}^3$ .

## 2.3 | PET and MRI preprocessing

For structural MRI, cortical surface modeling of the common space was performed using FreeSurfer image analysis suite v7.1.1 (<http://surfer.nmr.mgh.harvard.edu>). Cortical gray matter signal intensities were obtained by creating a surface in the interior of the cortical ribbon 40% starting from the gray matter/white matter border and projecting towards the gray matter/cerebrospinal fluid border. White matter intensities were sampled at 1 mm subjacent to the gray/white matter border. Ratios of gray/white matter intensity were created at each cortical surface vertex. After calculation of the ratio features, values were smoothed with a Gaussian kernel of 5 mm in FWHM for analysis utilizing a surface-based smoothing procedure that averaged data across neighboring cortical locations.

FBP-PET images were analyzed by an automatic pipeline to extract voxel-wise standardized uptake value ratios (SUVs) implemented in PETSURFER (<https://surfer.nmr.mgh.harvard.edu/fswiki/PetSurfer>). Structural images were used as the high-resolution template to run the partial volume correction (PVC) methods. The PET/anatomical image registration was performed and visually checked. Then we applied the extended three-compartment model (Muller-Gartner method) for PVC, using the whole cerebellum as the reference region. SUVs of the gray matter were finally sampled onto the brain surface in the common space and then smoothed on the two-dimensional surface by a Gaussian kernel of 5 mm in FWHM.

## 2.4 | Statistics

For the cross-sectional dataset, the demographic characteristics were compared using analysis of variance (ANOVA) or Chi-square test for continuous or nominal variables, respectively. We used analysis of covariance (ANCOVA) as the general linear model (GLM) to adjust age, global cortical thickness, and hippocampus volumes when comparing vertex-wise group differences in GWR. All the following analysis for GWR were adjusted for age. To evaluate the GWR along different stages in the AD continuum (i.e., MCI A $\beta$ + and AD A $\beta$ +), GLM was also used for vertex-wise correlation analyses between

cognitive performance and GWR after controlling for age and sex. An additional GLM was evaluated to assess vertex-wise variation in GWR and A $\beta$  SUVR. We tested the effect of cognitive impairment on GWR while controlling for the A $\beta$  SUVR at each vertex along the cortical mantle.

Repeated measures ANCOVA was used to assess cognition and GWR changes in the ADNI longitudinal dataset. To minimize the effect of aging, the time interval between visits was set as a covariate. All significant results in the GLMs went through cluster-wise correction for multiple comparisons by 10,000 permutations (Greve & Fischl, 2018). The significance of two-sided  $p < .05$  at cluster level after the correction was used in vertex-wise analyses unless stated elsewhere.

## 3 | RESULTS

### 3.1 | Demographics

A total of 184 participants were included in the cross-sectional dataset with six groups: CN A $\beta$ - and CN A $\beta$ +; MCI A $\beta$ - and MCI A $\beta$ +; Dementia A $\beta$ - and AD A $\beta$ +. Detailed demographics and cognitive characteristics were presented in Table 1. The participants of MCI A $\beta$ - and MCI A $\beta$ + had similar age and global cognitive performance ( $p = .724$  for age;  $p = .100$  for MoCA;  $p = .184$  for ACER), as well as Dementia A $\beta$ - and AD A $\beta$  + ( $p = .661$  for age;  $p = .194$  for MoCA; and  $p = .517$  for ACER). The participants in CN A $\beta$ + were elder than those of CN A $\beta$ - ( $p = .011$ ), and had worse performance in MoCA ( $p < .001$ ) and ACER ( $p = .025$ ).

### 3.2 | Cross-sectional GWR comparisons

As expected, compared to CN A $\beta$ -, MCI A $\beta$ + group had higher GWR throughout the portions of the inferior and superior temporal cortex as well as the right fusiform gyrus. In AD A $\beta$ +, more diffused regions showed higher GWR, including bilateral fusiform, temporal, superior frontal, and cingulate cortex. Lower GWR was found in the bilateral lingual cortex (Figure 1). The results indicated that GWR was able to discriminate AD-related cognitively impaired patients (AD A $\beta$ + and MCI A $\beta$ +) from healthy controls.

The comparisons between different A $\beta$  positivity in subjects with different levels of cognitive impairment (AD A $\beta$ + vs. Dementia A $\beta$ -; MCI A $\beta$ + vs. MCI A $\beta$ -) showed few differences in GWR. The AD A $\beta$ + and Dementia A $\beta$ - had no significant differences in vertex-wise GWR comparison, neither did MCI A $\beta$ + and MCI A $\beta$ - groups. Among the control participants (including CN A $\beta$ + and CN A $\beta$ -), the GWR and amyloid did not show significant correlation in the vertex-wise analysis after multiple comparison correction, although CN A $\beta$ + showed higher GWR in left para-hippocampal gyrus than CN A $\beta$ -.

For cortical thickness, only AD A $\beta$ + showed thinner cortical thickness than AD A $\beta$ - in the right precentral and lingual cortex, while no differences were observed between MCI A $\beta$ + and MCI A $\beta$ -, nor CN A $\beta$ + and CN A $\beta$ -.

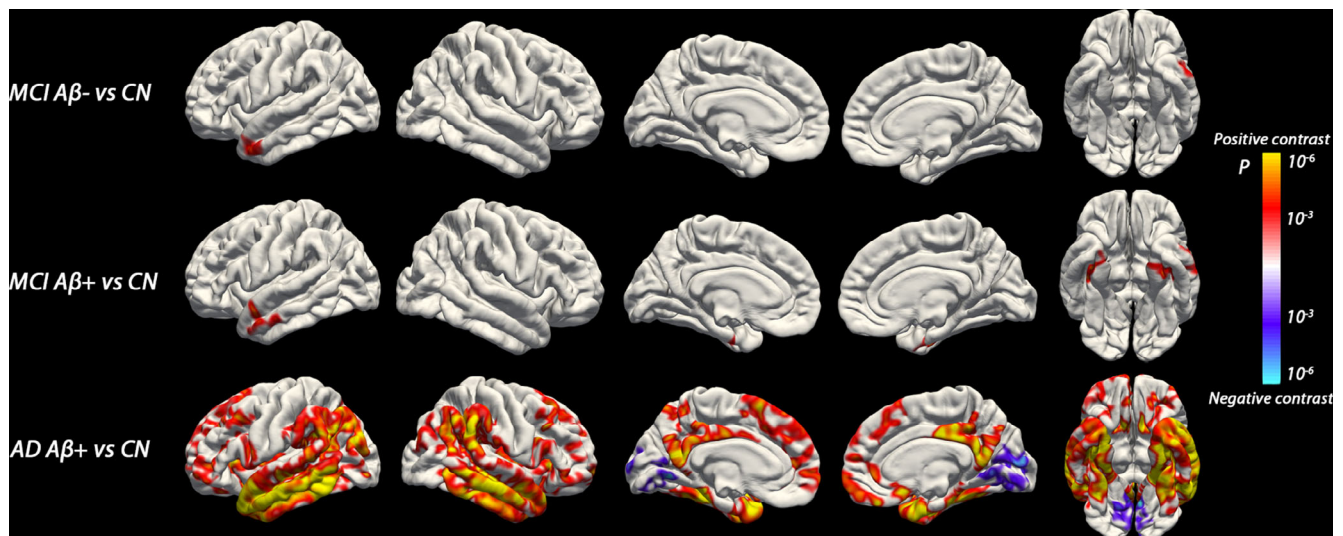


**FIGURE 1** Between-group differences in GWR (in the cross-sectional dataset). Effects of MCI A $\beta$ -, MCI A $\beta$ +, and AD A $\beta$ + on GWR are shown respectively. Only the significant clusters with corrected  $p < .05$  after permutations are colored. The color bar represents uncorrected  $p$  values. Positive  $p$  represents a positive difference in the contrast and vice versa. AD A $\beta$ +, dementia with A $\beta$  positivity; CN, cognitively normal participants without A $\beta$  deposition; GWR, gray/white signal intensity ratio; MCI A $\beta$ +, mild cognitive impairment with A $\beta$  positivity.

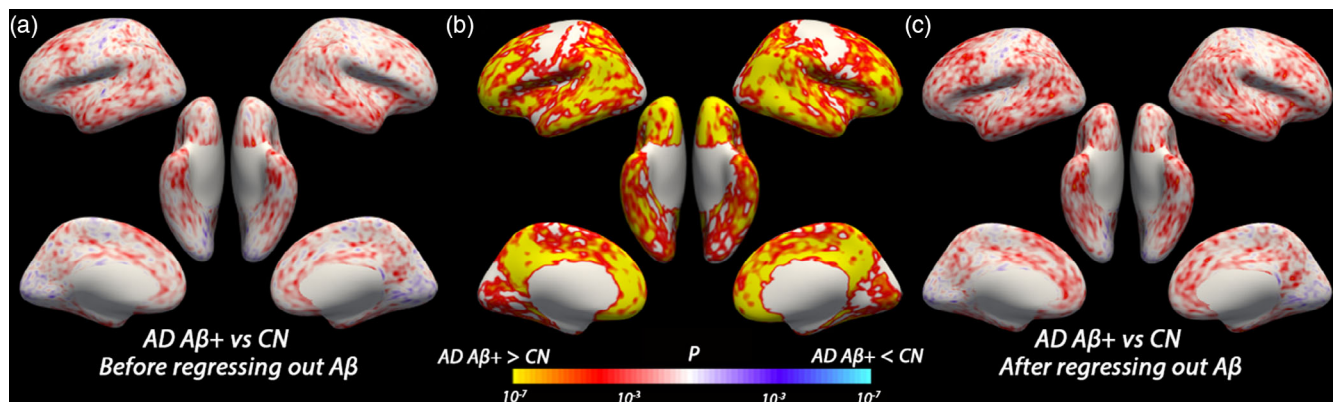


**FIGURE 2** Effect of AD A $\beta$ + on GWR with and without controlling for A $\beta$  deposition. Effects of AD A $\beta$ + on GWR (a), A $\beta$  deposition measured with PET (b), and GWR after controlling for A $\beta$  SUVR at each vertex along the cortex (c) are shown. The color bar represents uncorrected  $p$  values. Positive  $p$  values represent a positive difference in the contrast. AD A $\beta$ +, dementia with A $\beta$  positivity; CN, cognitively normal participants without A $\beta$  deposition; GWR, gray/white signal intensity ratio.

### 3.3 | Association between GWR and $\beta$ -amyloid

We performed direct vertex-wise correlation analysis between GWR and A $\beta$  deposition across clinical participants with positive A $\beta$  (i.e., AD A $\beta$ + and MCI A $\beta$ +,  $N = 88$ ), and across all 184 participants. No cortical cluster of significant correlation was found in either population.

For further validation, we evaluated the effect of A $\beta$  on GWR difference between CN and AD A $\beta$ + participants. Figure 2a showed the same results as the third row of Figure 1 but with stretched inflated surface of brain so as to show results more completely. Following Figure 2b showing the A $\beta$  deposition in AD A $\beta$ +, Figure 2c demonstrated similar pattern of higher GWR in AD A $\beta$ + after adjustment for the A $\beta$  SUVR at each vertex along the cortical mantle (uncorrected

$p$  values were used to show the pattern of group difference). These results suggested that the effects of cognitive impairment on GWR were beyond the variance accounted by A $\beta$  deposit alone.

### 3.4 | Association between GWR and cognition

There were strong associations between multiple cognitive tests and GWR across the clinical participants: MCI A $\beta$ + and AD A $\beta$ + ( $N = 88$ ). The global cognition assessed by ACER was negatively correlated with GWR in the left temporal pole and entorhinal cortex. Meanwhile, there were positive correlations between ACER and GWR in the bilateral lingual gyrus and primary motor cortex (Figure 3, left column). To

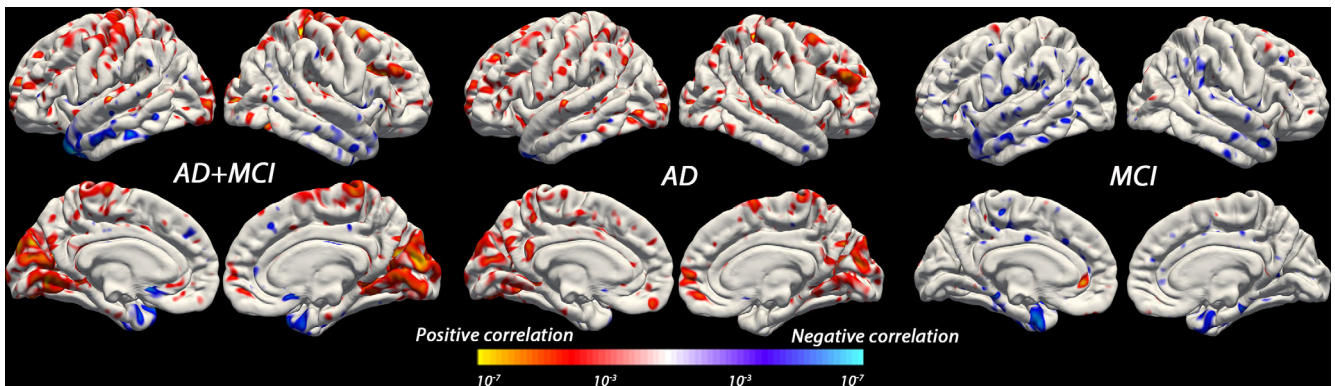


**FIGURE 3** Correlation between GWR and ACER across all clinical participants in MCI A $\beta$ + and AD A $\beta$ +, AD A $\beta$ +, and MCI A $\beta$ +, respectively. The color bar represents uncorrected  $p$  values. Negative  $p$  values represent negative correlation and vice versa. ACER, Addenbrooke's Cognitive Examination-Revised; AD, dementia with A $\beta$  positivity; GWR, gray/white signal intensity ratio; MCI, mild cognitive impairment with A $\beta$  positivity.

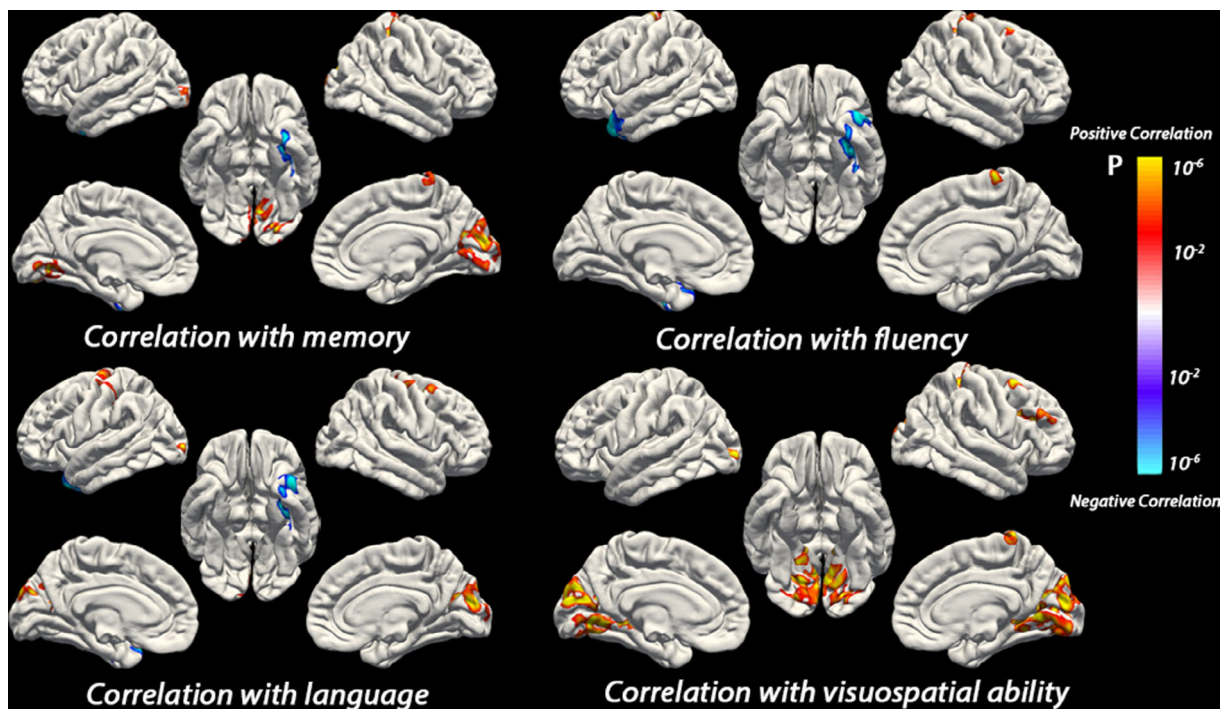


**FIGURE 4** Correlation between GWR and subtests of ACER across all clinical participants in MCI A $\beta$ + and AD A $\beta$ +. Only the significant clusters with corrected  $p < .05$  after permutations were colored. The color bar represents uncorrected  $p$  values. Negative  $p$  values represent negative correlation and vice versa. ACER, Addenbrooke's Cognitive Examination-Revised; AD A $\beta$ +, dementia with A $\beta$  positivity; GWR, gray/white signal intensity ratio; MCI A $\beta$ +, mild cognitive impairment with A $\beta$  positivity.

avoid false correlation due to group difference, correlation map was illustrated between ACER and GWR in AD A $\beta$  and MCI A $\beta$ , respectively (Figure 3, middle and right column). Uncorrected  $p$  values were used in Figure 3 to show the pattern. The negative correlation between ACER and GWR in the bilateral temporal cortex were observed in both AD and MCI, and it was more remarkable in the MCI A $\beta$  group.

The cognitive domains assessed by subtests of ACER had some specific patterns of a relationship with GWR to ACER total score. The

negative relationship in ACER–GWR association was mainly attributed to memory, language, and fluency as shown in Figure 4. These related negative changes were mainly distributed in the temporal pole and entorhinal cortex of dominant hemisphere (left hemisphere). We also observed remarkable positive correlations between visuospatial performance and GWR in the bilateral lingual and lateral occipital cortex (Figure 4).

By contrast, correlations between GWR and MoCA or ACER were not observed across participants of MCI A $\beta$  and Dementia A $\beta$  ( $N = 36$ ).

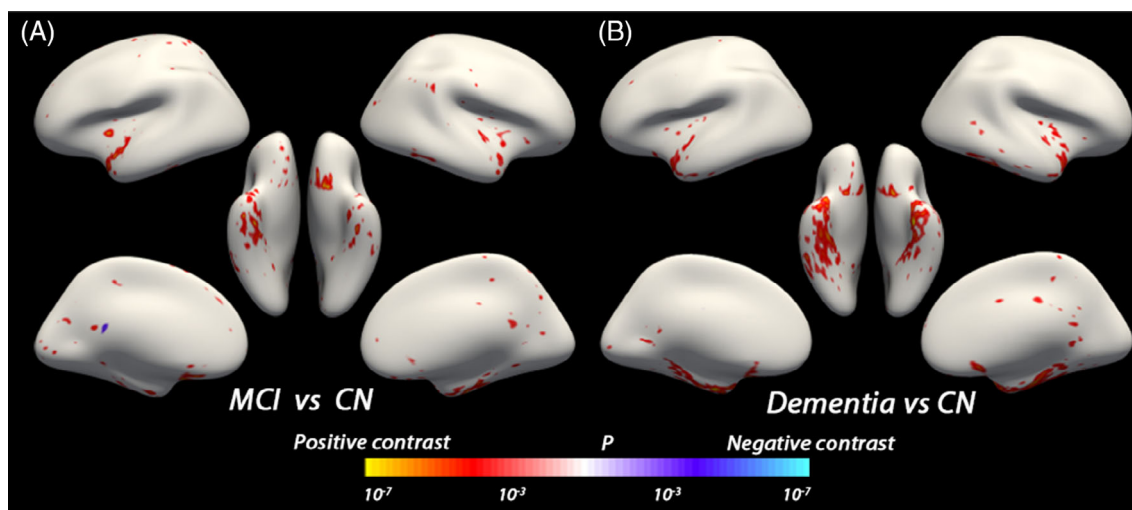


**FIGURE 5** Longitudinal changes in GWR in the development of AD. Repeated measures ANCOVA was used to determine if GWR changes over the course of the disease progression (CN to MCI to Dementia). The time interval between visits was set as a covariate. Stretched inflated surface of brain was used as template to show results deep in the sulcus clearly. Only the significant clusters with corrected  $p < .01$  after permutations were colored. The color bar represents uncorrected  $p$  values. Positive  $p$  values represent a positive difference in the contrast and vice versa. AD, dementia; CN, cognitively normal participants; GWR, gray/white signal intensity ratio; MCI, mild cognitive impairment.

**TABLE 3** Demographics and longitudinal cognitive assessments.

CN-MCI-Dementia	Visit 1, N = 26	Visit 2, N = 26	Visit 3, N = 26	$p$
MMSE	29.54 ± 0.71	27.35 ± 1.79**	24.58 ± 2.56**	<.001
ADAS-13	9.72 ± 4.5	16.73 ± 5.71**	24.72 ± 6.53**	<.001
RAVLT immediate	44.46 ± 8.74	37.96 ± 9.94*	27.58 ± 8.29**	<.001
RAVLT learning	5.88 ± 2.6	3.88 ± 2.57**	2.31 ± 1.83**	<.001
Time since baseline (months)	0	56.77 ± 29.06	86.77 ± 33.82	-
CN-CN-CN	Visit 1, N = 26	Visit 2, N = 26	Visit 3, N = 26	$p$
MMSE	29.08 ± 1.20	29.38 ± 0.98	29.00 ± 1.32	.344
ADAS-13	8.06 ± 3.96	8.54 ± 4.24	9.38 ± 4.64	.073
RAVLT immediate	44.46 ± 7.95	48.42 ± 11.61	49.19 ± 10.50	.016
RAVLT learning	6.35 ± 2.67	5.65 ± 2.70	5.27 ± 2.44	.226
Time since baseline (months)	0	60.47 ± 1.01	109.53 ± 4.10	-

Note: Values represented mean ± standard deviation unless otherwise specified. \*\* $p < .001$ , \* $p < .01$  identified between MCI versus CN, Dementia versus CN. Bonferroni adjustment for multiple comparison. Abbreviations: ADAS, Alzheimer's Disease Assessment Scale; CN, cognitively normal participants; MCI, mild cognitive impairment; MMSE, Mini-Mental State Examination; RAVLT, Rey Auditory Verbal Learning Test.

### 3.5 | Longitudinal GWR changes

To explore the longitudinal GWR changes in the disease progression from CN to MCI and then to dementia, we investigated the ADNI dataset and included individuals with a diagnosis of CN  $A\beta^-$  at baseline, then MCI, and finally dementia  $A\beta^+$  in the follow-up. For control, we included the same number of matched participants that remained CN  $A\beta^-$  throughout the follow-up. There were 26 participants in the CN-MCI-Dementia group who completed all three visits with valid data (MRI and cognitive scores). Participants were assessed with MMSE, Alzheimer's Disease Assessment Scale (ADAS)-13, and Rey

Auditory Verbal Learning Test (RAVLT) over the course of disease progression (Table 2). The group comparison between the CN-CN-CN and CN-MCI-AD at baseline when they were all diagnosed as normal showed no difference in GWR.

When individuals progressed from CN to MCI, the GWR increased mainly in the left fusiform, inferior/superior temporal, and entorhinal cortex, as well as the right superior temporal, entorhinal, and medial orbitofrontal cortex. After progression to dementia, the increased GWR was observed in larger cortical regions covering bilateral temporal lobes, entorhinal cortex, and left para-hippocampal gyrus (Figure 5). In the CN-CN-CN group (Table 3), all participants

had stable cognitive performance in the longitudinal visits and did not show GWR changes during the visits.

## 4 | DISCUSSION

In the present study, increased GWR was observed in the temporal cortex in both MCI and AD from both cross-sectional and longitudinal datasets. Furthermore, as dementia progressed, a notable increase in GWR was observed in the temporal and entorhinal cortex. These changes in GWR were found to be associated with cognitive performance across multiple domains in individuals with underlying A $\beta$  pathology, but not with A $\beta$  positivity/deposition directly.

Prior research has shown that GWR is influenced by aging and cognitive decline. Salat et al. (2009) discovered that GWR significantly varied with increasing age throughout adulthood, showing distinctions between cognitively demented and nondemented individuals. In our previous research (Li et al., 2020), augmented GWR in AD was observed after detrending the ages. This finding establishes a clear correlation between the extent of dementia and the increase in GWR, thereby highlighting the potential value of GWR in clinical practice for the diagnosis and assessment of AD progression.

GWR can serve as a novel biomarker of neurodegeneration in addition to traditional structure imaging biomarkers such as cortical thickness. We found that GWR alterations probably took place at an earlier stage of disease independent of cortical atrophy. As our cross-sectional study showed, cortical atrophy was detected only in the AD A $\beta$ + group, but GWR alterations were observed in both MCI A $\beta$ + and AD A $\beta$ + groups. As a result, this study offers new evidence supporting GWR as an imaging marker that is sensitive to cognitive impairment. GWR has the advantage of detecting cognitive impairment earlier than conventional neuroimaging parameters like cortical thickness and hippocampal atrophy, as it measures tissue signal properties rather than tissue integrity (Salat et al., 2009). GWR alterations may be attributed to changes in the microstructure of brain tissue, reflecting alterations in the water and lipid content of both gray and white matter. (Jefferson et al., 2015).

Our study aimed to investigate the relationship between GWR and cognitive decline in individuals, but it is important to note that our findings differed from some previous studies. A previous research conducted by Jefferson et al. (2015) found that decreased baseline GWR could discriminate between MCI patients who later developed dementia and those who did not, which was found to be independent of cortical thickness or hippocampal volume. In contrast, we observed an increase in GWR from CN to MCI individuals, and further to those with AD. This discrepancy might be explained by methodological differences between our studies. In Jefferson (2015), the researchers acquired MRI data at baseline and subsequently followed the MMSE scores of subjects to identify MCI converters. Although this study design was reasonable for investigating the predictive value of GWR at baseline, it did not allow for the assessment of GWR differences between MCI converters and non-converters at the end point. To overcome this limitation, our study used both cross-sectional and

longitudinal datasets to examine the relationship between GWR and cognition at the same time point (cross-sectional dataset), as well as to track the changes in GWR during the progression of AD (longitudinal dataset). These differences in study design may also partially explain the lack of significant differences in baseline GWR between individuals with stable cognition (CN–CN–CN group) and those with cognitive decline (CN–MCI–Dementia group).

In another recent cross-sectional study, it was found that GWR decreased in atypical syndromes of AD (primary progressive aphasia and posterior cortical atrophy) (Putcha et al., 2023). This suggests that GWR change may vary across different brain regions. Specifically, we observed a decrease in GWR in the bilateral lingual cortex of AD, which is part of the posterior cortex. These different patterns of GWR change may be attributed to different disease phenotypes. It is important to note that our study primarily focused on amnesic AD in a larger cohort. In addition, our extended protocol examined correlation between GWR and tau accumulation. In 47 subjects with tau PET across clinical patients (AD A $\beta$ + and MCI A $\beta$ +), GWR showed a positive correlation with tau in the left supramarginal and lateral occipital gyrus, as well as the right middle frontal cortex (Figure S1). The partially overlapped spatial pattern of GWR and tau deposit, which was consistent with the prior study (Putcha et al., 2023), suggesting that GWR alteration was possibly related to the biological process underlying tau accumulation. This finding indicates GWR could potentially be a neurodegenerative feature of AD. More details can be found in Appendix S1.

Meanwhile, our study analyzed the topographic patterns of GWR alterations in individuals with different cognitive performances. In individuals with MCI, a significant increase of GWR was identified in the temporal cortex and fusiform gyrus. In patients with AD, more diffused changes of GWR were detected in the bilateral temporal cortex, frontal cortex, precuneus, and cingulate cortex. This finding is consistent with a previous study that reported GWR alterations in medial and lateral temporal cortex in AD (Salat et al., 2011). Moreover, when examining the correlation between regional specific changes in GWR and cognitive performance, we found that global cognition was related to the left temporal pole and entorhinal cortex in both MCI A $\beta$ + and AD A $\beta$ + patients. The negative relationship in ACER–GWR association was mainly attributed to memory, language, and fluency.

The temporal lobe, a well-documented area affected in AD pathology and strongly correlated with cognitive performance (Scheltens et al., 1992), may show early pathological changes at the initial stage of AD pathogenesis. This finding was further supported by similar regional specific cortex atrophy and A $\beta$  deposit verified by structure MRI and Pittsburgh compound B PET (Doré et al., 2013). Additionally, our observations indicated that CN A $\beta$ + individuals displayed higher GWR in the left para-hippocampal gyrus than CN A $\beta$ – individuals. A prevalence study demonstrated that the incident amnesic MCI risk increased more than 2-fold in CN A $\beta$ + individuals compared to CN A $\beta$ – individuals. The risk of AD dementia was found to be 2.56-fold higher for CN and aMCI A $\beta$ + individuals compared to those who were amyloid negative (Roberts et al., 2018). These results, together with our findings, suggested that the temporal and

entorhinal cortex may undergo early pathological changes during the initial stage of AD pathogenesis.

In order to investigate the regional correlation between GWR and A $\beta$  deposition, vertex-wise correlation analysis was performed across all participants ( $N = 184$ ) and clinical participants with positive A $\beta$  (i.e., AD A $\beta$ + and MCI A $\beta$ +,  $N = 88$ ). However, the results of this analysis failed to show any significant correlation, indicating that GWR and A $\beta$  SUVR were not directly dependent on each other topologically in each brain region. These findings, however, do not rule out the potential relationship between GWR and A $\beta$ . Previous preclinical research has demonstrated that local A $\beta$  deposit could initiate distant dysfunction (Deleglise et al., 2014). As neurons are highly polarized, and axonal and synaptic dysfunctions can occur long before somatic cell death (Scheff et al., 2007; Terry, 2000), it is possible that A $\beta$  and tau stress can propagate within neuron or even transgress neurons through the neuronal network. Based on this theory, a recent study used  $\mu$ FD-based reconstructed neuronal networks to demonstrate that local A $\beta$  deposit causes distant neurotransmission disturbance, which plays a role in the early progression of AD (Deleglise et al., 2014). Therefore, these findings may help explain why cognition was related to GWR alterations in the left temporal pole and entorhinal cortex only among A $\beta$ + patients, whereas no interaction was noted between local A $\beta$  deposit and GWR through vertex-wise correlation analysis.

In addition to our cross-sectional findings, the current study also included a subset of patients in the ADNI dataset that revealed a complete disease course of the AD continuum. Compared with mounting evidence focused on AD, few studies have specifically investigated the pre-MCI stage (Apostolova et al., 2010; Jack et al., 2005; Smith et al., 2007). However, based on current knowledge, brain volume loss begins years before the emergence of clinical symptoms in MCI (Carmichael et al., 2009). Certain brain structural changes, such as decreased gray matter volume in the hippocampus (Apostolova et al., 2010), anteromedial temporal lobe, and left angular gyrus (Smith et al., 2007), as well as rates of ventricle atrophy (Jack et al., 2005) have been associated with a higher risk of MCI. These findings suggest that brain structure changes prior to the development of MCI. Therefore, it is reasonable to assume that microstructure alterations, as revealed by GWR, are initiated even earlier during the pre-MCI stage. To further investigate the disease course of the AD continuum, our study included a subset of patients in the ADNI dataset who were initially classified as A $\beta$ - cognitively normal individuals but were subsequently diagnosed with MCI and later A $\beta$ + AD during follow-up. This longitudinal cohort, with a mean baseline age of 75 and 50% of participants carrying ApoE  $\epsilon$ 4 (Table 2), provided insights into the longitudinal changes of GWR during the progression of AD. Moreover, it is important to note that the duration of each stage in AD was influenced by age, sex, and APOE genotype (Vermunt et al., 2019). For subjects aged 75 with ApoE  $\epsilon$ 4, the duration from CN to MCI was 2–6 years and the duration from MCI to dementia was around 2.5 years. For subjects aged 75 without ApoE  $\epsilon$ 4, the durations from CN to MCI, and from MCI to dementia were 3–10 years and 4–5 years. In our study, the mean time interval was

4.7 years from CN to MCI and 2.5 years from MCI to dementia, which aligns with the previous research.

The major limitation of the current study was the lack of sufficient follow-up to identify converters and non-converters. Instead, we used the FBP tracer to classify the subjects as A $\beta$ + or A $\beta$ - to discriminate between AD-associated MCI and non-AD-associated MCI. However, some individuals with A $\beta$  deposit at death did not present with the cognitive issue throughout their whole lifetime (Grøntvedt et al., 2018). In addition, the small sample size of controls A $\beta$ + and Dementia A $\beta$ - limited statistical power of comparisons involving the two groups. Therefore, the absence of correlation between cognition and GWR in A $\beta$ - patients may result from the power issue. Future studies with larger sample size are required to further investigate the correlation between GWR and cognitive performance in the dementia A $\beta$ - population.

## 5 | CONCLUSION

The findings of the current study suggest that GWR alterations are correlated with cognitive decline during the pathogenesis of  $\beta$ -amyloid in MCI and AD. It was observed that the spatial pattern of GWR-increased regions was not significantly influenced by  $\beta$ -amyloid deposits. These results demonstrated that GWR can serve as an imaging biomarker of neurodegeneration in AD using standard T1-weighted brain images without the need for additional procedures or costs to the standard of care.

### AUTHOR CONTRIBUTIONS

**Xiaomeng Xu:** Data curation, investigation, writing—original draft preparation. **Ikbeom Jang:** Methodology, writing—reviewing and editing. **Junfang Zhang:** Writing—reviewing and editing. **Miao Zhang:** Project administration, validation. **Lijun Wang:** Investigation, data curation. **Guanyu Ye:** Investigation, data curation. **Aonan Zhao:** Investigation, data curation. **Yichi Zhang:** Investigation, data curation. **Biao Li:** Supervision, project administration. **Jun Liu:** Supervision, writing—reviewing and editing. **Binyin Li:** Supervision, conceptualization, methodology, writing—original draft preparation, reviewing and editing.

### ACKNOWLEDGMENTS

We would like to thank our anonymous reviewers for their thoughtful comments on the manuscript. We are also grateful to all research participants. We thank Pro. Hank Kung and Lin Zhu for their kindly gifting of Florbetapir precursor and suggestions to improve this manuscript. This work was supported by Hankuk University of Foreign Studies Research Fund of 2023. We are also grateful to all of the study participants for their patience and cooperation.

Data collection and sharing for ADNI in the study was funded by the Alzheimer's Disease Neuroimaging Initiative (ADNI) (National Institutes of Health Grant U01 AG024904) and DOD ADNI (Department of Defense award number W81XWH-12-2-0012). ADNI is funded by the National Institute on Aging, the National Institute of Biomedical Imaging and Bioengineering, and through generous

contributions from the following: AbbVie, Alzheimer's Association; Alzheimer's Drug Discovery Foundation; Araclon Biotech; BioClinica, Inc.; Biogen; Bristol-Myers Squibb Company; CereSpir, Inc.; Cogstate; Eisai Inc.; Elan Pharmaceuticals, Inc.; Eli Lilly and Company; EuroImmun; F. Hoffmann-La Roche Ltd and its affiliated company Genentech, Inc.; Fujirebio; GE Healthcare; IXICO Ltd.; Janssen Alzheimer Immunotherapy Research & Development, LLC.; Johnson & Johnson Pharmaceutical Research & Development LLC.; Lumosity; Lundbeck; Merck & Co., Inc.; Meso Scale Diagnostics, LLC.; NeuroRx Research; Neurotrack Technologies; Novartis Pharmaceuticals Corporation; Pfizer Inc.; Piramal Imaging; Servier; Takeda Pharmaceutical Company; and Transition Therapeutics. The Canadian Institutes of Health Research is providing funds to support ADNI clinical sites in Canada. Private sector contributions are facilitated by the Foundation for the National Institutes of Health ([www.fnih.org](http://www.fnih.org)). The grantee organization is the Northern California Institute for Research and Education, and the study is coordinated by the Alzheimer's Therapeutic Research Institute at the University of Southern California. ADNI data are disseminated by the Laboratory for Neuro Imaging at the University of Southern California.

#### FUNDING INFORMATION

The trial is supported by the Shanghai Rising-Star Program (21QA1405800), the National Natural Science Foundation of China (82271441 and 81901180).

#### CONFLICT OF INTEREST STATEMENT

None.

#### DATA AVAILABILITY STATEMENT

For inquiries or opportunities for working with our cross-sectional data, please contact the corresponding author. The ADNI data used in the preparation of this article were obtained from the Alzheimer's Disease Neuroimaging Initiative (ADNI) database ([adni.loni.usc.edu](http://adni.loni.usc.edu)). As such, the investigators within the ADNI contributed to the design and implementation of ADNI and/or provided data but did not participate in the analysis or writing of this report.

#### ORCID

Xiaomeng Xu  <https://orcid.org/0000-0002-1717-538X>

Binyin Li  <https://orcid.org/0000-0003-1953-382X>

#### REFERENCES

- Apostolova, L. G., Mosconi, L., Thompson, P. M., Green, A. E., Hwang, K. S., Ramirez, A., Mistur, R., Tsui, W. H., & de Leon, M. J. (2010). Subregional hippocampal atrophy predicts Alzheimer's dementia in the cognitively normal. *Neurobiology of Aging*, 31, 1077–1088. <https://doi.org/10.1016/j.neurobiolaging.2008.08.008>
- Carmichael, O. T., Lopez, O., Becker, J. T., & Kuller, L. (2009). Trajectories of brain loss in aging and the development of cognitive impairment. *Neurology*, 72, 771; author reply 771–772–772. <https://doi.org/10.1212/01.wnl.0000339386.26096.93>
- Deleglise, B., Magnifico, S., Duplus, E., Vaur, P., Soubeyre, V., Belle, M., Vignes, M., Viovy, J.-L., Jacotot, E., Peyrin, J.-M., & Brugg, B. (2014).  $\beta$ -Amyloid induces a dying-back process and remote trans-synaptic alterations in a microfluidic-based reconstructed neuronal network. *Acta Neuropathologica Communications*, 2, 145. <https://doi.org/10.1186/s40478-014-0145-3>
- Doré, V., Villemagne, V. L., Bourgeat, P., Frapp, J., Acosta, O., Chetelat, G., Zhou, L., Martins, R., Ellis, K. A., Masters, C. L., Ames, D., Salvado, O., & Rowe, C. C. (2013). Cross-sectional and longitudinal analysis of the relationship between A $\beta$  deposition, cortical thickness, and memory in cognitively unimpaired individuals and in Alzheimer disease. *JAMA Neurology*, 70, 903–911. <https://doi.org/10.1001/jamaneuro.2013.1062>
- Fang, R., Wang, G., Huang, Y., Zhuang, J.-P., Tang, H.-D., Wang, Y., Deng, Y.-L., Xu, W., Chen, S.-D., & Ren, R.-J. (2014). Validation of the Chinese version of Addenbrooke's cognitive examination-revised for screening mild Alzheimer's disease and mild cognitive impairment. *Dementia and Geriatric Cognitive Disorders*, 37, 223–231. <https://doi.org/10.1159/000353541>
- Greve, D. N., & Fischl, B. (2018). False positive rates in surface-based anatomical analysis. *NeuroImage*, 171, 6–14. <https://doi.org/10.1016/j.neuroimage.2017.12.072>
- Grøntvedt, G. R., Schröder, T. N., Sando, S. B., White, L., Bråthen, G., & Doeller, C. F. (2018). Alzheimer's disease. *Current Biology*, 28, R645–R649. <https://doi.org/10.1016/j.cub.2018.04.080>
- Grydeland, H., Westlye, L. T., Walhovd, K. B., & Fjell, A. M. (2013). Improved prediction of Alzheimer's disease with longitudinal white matter/gray matter contrast changes. *Human Brain Mapping*, 34, 2775–2785. <https://doi.org/10.1002/hbm.22103>
- Jack, C. R., Bennett, D. A., Blennow, K., Carrillo, M. C., Dunn, B., Haeberlein, S. B., Holtzman, D. M., Jagust, W., Jessen, F., Karlawish, J., Liu, E., Molinuevo, J. L., Montine, T., Phelps, C., Rankin, K. P., Rowe, C. C., Scheltens, P., Siemers, E., Snyder, H. M., & Sperling, R. (2018). NIA-AA research framework: Toward a biological definition of Alzheimer's disease. *Alzheimer's & Dementia*, 14, 535–562. <https://doi.org/10.1016/j.jalz.2018.02.018>
- Jack, C. R., Shiung, M. M., Weigand, S. D., O'Brien, P. C., Gunter, J. L., Boeve, B. F., Knopman, D. S., Smith, G. E., Ivnik, R. J., Tangalos, E. G., & Petersen, R. C. (2005). Brain atrophy rates predict subsequent clinical conversion in normal elderly and amnesic MCI. *Neurology*, 65, 1227–1231. <https://doi.org/10.1212/01.wnl.0000180958.22678.91>
- Jang, I., Li, B., Riphagen, J. M., Dickerson, B. C., & Salat, D. H. (2022). Multi-scale structural mapping of Alzheimer's disease neurodegeneration. *NeuroImage: Clinical*, 33, 102948. <https://doi.org/10.1016/j.nicl.2022.102948>
- Jefferson, A. L., Gifford, K. A., Damon, S., Chapman, G. W., Liu, D., Sparling, J., Dobromyslin, V., Salat, D., & Alzheimer's Disease Neuroimaging Initiative. (2015). Gray & white matter tissue contrast differentiates mild cognitive impairment converters from non-converters. *Brain Imaging and Behavior*, 9, 141–148. <https://doi.org/10.1007/s11682-014-9291-2>
- Katzman, R., Zhang, M. Y., Qu, O., Wang, Z. Y., Liu, W. T., Yu, E., Wong, S. C., Salmon, D. P., & Grant, I. (1988). A Chinese version of the Mini-Mental State Examination; impact of illiteracy in a Shanghai dementia survey. *Journal of Clinical Epidemiology*, 41, 971–978. [https://doi.org/10.1016/0895-4356\(88\)90034-0](https://doi.org/10.1016/0895-4356(88)90034-0)
- Kim, D. M., Xanthakos, S. A., Tupler, L. A., Barboriak, D. P., Charles, H. C., MacFall, J. R., & Krishnan, K. R. R. (2002). MR signal intensity of gray matter/white matter contrast and intracranial fat: Effects of age and sex. *Psychiatry Research*, 114, 149–161. [https://doi.org/10.1016/S0925-4927\(02\)00024-0](https://doi.org/10.1016/S0925-4927(02)00024-0)
- Landau, S. M., Mintun, M. A., Joshi, A. D., Koeppe, R. A., Petersen, R. C., Aisen, P. S., Weiner, M. W., Jagust, W. J., & Alzheimer's Disease Neuroimaging Initiative. (2012). Amyloid deposition, hypometabolism, and longitudinal cognitive decline. *Annals of Neurology*, 72, 578–586. <https://doi.org/10.1002/ana.23650>
- Li, B., Jang, I., Riphagen, J., Almkatoum, R., Yochim, K. M., Ances, B. M., Bookheimer, S. Y., Salat, D. H., & Alzheimer's Disease Neuroimaging, I.

- (2021). Identifying individuals with Alzheimer's disease-like brains based on structural imaging in the Human Connectome Project Aging cohort. *Human Brain Mapping*, 42, 5535–5546. <https://doi.org/10.1002/hbm.25626>
- Li, B., Zhang, M., Jang, I., Ye, G., Zhou, L., He, G., Lin, X., Meng, H., Huang, X., Hai, W., Chen, S., Li, B., & Liu, J. (2021). Amyloid-Beta influences memory via functional connectivity during memory retrieval in Alzheimer's disease. *Frontiers in Aging Neuroscience*, 13, 721171. <https://doi.org/10.3389/fnagi.2021.721171>
- Li, B., Zhang, M., Riphagen, J., Morrison Yochim, K., Li, B., Liu, J., Salat, D. H., & Alzheimer's Disease Neuroimaging, I. (2020). Prediction of clinical and biomarker conformed Alzheimer's disease and mild cognitive impairment from multi-feature brain structural MRI using age-correction from a large independent lifespan sample. *Neuroimage: Clinical*, 28, 102387. <https://doi.org/10.1016/j.nicl.2020.102387>
- Putcha, D., Katsumi, Y., Brickhouse, M., Flaherty, R., Salat, D. H., Touroutoglou, A., & Dickerson, B. C. (2023). Gray to white matter signal ratio as a novel biomarker of neurodegeneration in Alzheimer's disease. *NeuroImage: Clinical*, 37, 103303. <https://doi.org/10.1016/j.nicl.2022.103303>
- Roberts, R. O., Aakre, J. A., Kremers, W. K., Vassilaki, M., Knopman, D. S., Mielke, M. M., Alhurani, R., Geda, Y. E., Machulda, M. M., Coloma, P., Schauble, B., Lowe, V. J., Jack, C. R., & Petersen, R. C. (2018). Prevalence and outcomes of amyloid positivity among persons without dementia in a longitudinal, population-based setting. *JAMA Neurology*, 75, 970–979. <https://doi.org/10.1001/jamaneuro.2018.0629>
- Salat, D. H., Chen, J. J., van der Kouwe, A. J., Greve, D. N., Fischl, B., & Rosas, H. D. (2011). Hippocampal degeneration is associated with temporal and limbic gray matter/white matter tissue contrast in Alzheimer's disease. *NeuroImage*, 54, 1795–1802. <https://doi.org/10.1016/j.neuroimage.2010.10.034>
- Salat, D. H., Lee, S. Y., van der Kouwe, A. J., Greve, D. N., Fischl, B., & Rosas, H. D. (2009). Age-associated alterations in cortical gray and white matter signal intensity and gray to white matter contrast. *NeuroImage*, 48, 21–28. <https://doi.org/10.1016/j.neuroimage.2009.06.074>
- Scheff, S. W., Price, D. A., Schmitt, F. A., DeKosky, S. T., & Mufson, E. J. (2007). Synaptic alterations in CA1 in mild Alzheimer disease and mild cognitive impairment. *Neurology*, 68, 1501–1508. <https://doi.org/10.1212/01.wnl.0000260698.46517.8f>
- Scheltens, P., Leys, D., Barkhof, F., Huglo, D., Weinstein, H. C., Vermersch, P., Kuiper, M., Steinling, M., Wolters, E. C., & Valk, J. (1992). Atrophy of medial temporal lobes on MRI in “probable” Alzheimer's disease and normal ageing: Diagnostic value and neuropsychological correlates. *Journal of Neurology, Neurosurgery, and Psychiatry*, 55, 967–972. <https://doi.org/10.1136/jnnp.55.10.967>
- Smith, C. D., Chebrolu, H., Wekstein, D. R., Schmitt, F. A., Jicha, G. A., Cooper, G., & Markesbery, W. R. (2007). Brain structural alterations before mild cognitive impairment. *Neurology*, 68, 1268–1273. <https://doi.org/10.1212/01.wnl.0000259542.54830.34>
- Terry, R. D. (2000). Cell death or synaptic loss in Alzheimer disease. *Journal of Neuropathology and Experimental Neurology*, 59, 1118–1119. <https://doi.org/10.1093/jnen/59.12.1118>
- Vermunt, L., Sikkes, S. A. M., van den Hout, A., Handels, R., Bos, I., van der Flier, W. M., Kern, S., Ousset, P.-J., Maruff, P., Skoog, I., Verhey, F. R. J., Freund-Levi, Y., Tsolaki, M., Wallin, Å. K., Olde Rikkert, M., Soininen, H., Spuru, L., Zetterberg, H., Blennow, K., ... ICTUS/DSA study groups. (2019). Duration of preclinical, prodromal, and dementia stages of Alzheimer's disease in relation to age, sex, and APOE genotype. *Alzheimer's & Dementia*, 15, 888–898. <https://doi.org/10.1016/j.jalz.2019.04.001>
- Westlye, L. T., Walhovd, K. B., Dale, A. M., Espeseth, T., Reinvang, I., Raz, N., Agartz, I., Greve, D. N., Fischl, B., & Fjell, A. M. (2009). Increased sensitivity to effects of normal aging and Alzheimer's disease on cortical thickness by adjustment for local variability in gray/white contrast: A multi-sample MRI study. *NeuroImage*, 47, 1545–1557. <https://doi.org/10.1016/j.neuroimage.2009.05.084>

## SUPPORTING INFORMATION

Additional supporting information can be found online in the Supporting Information section at the end of this article.

**How to cite this article:** Xu, X., Jang, I., Zhang, J., Zhang, M., Wang, L., Ye, G., Zhao, A., Zhang, Y., Li, B., Liu, J., Li, B., & for the Alzheimer's Disease Neuroimaging Initiative (2023). Cortical gray to white matter signal intensity ratio as a sign of neurodegeneration and cognition independent of  $\beta$ -amyloid in dementia. *Human Brain Mapping*, 1–11. <https://doi.org/10.1002/hbm.26532>